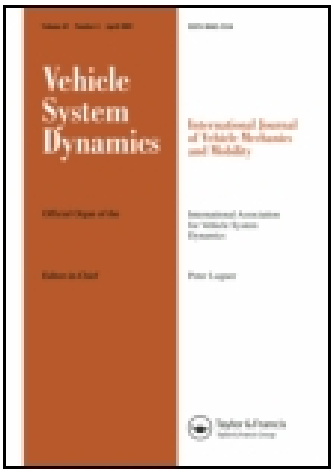

Vehicle System Dynamics: International Journal of Vehicle Mechanics and Mobility

Publication details, including instructions for authors and subscription information:
http://www.tandfonline.com/loi/nvsd20

Vehicle trajectory linearisation to enable efficient optimisation of the constant speed racing line

Julian P. Timings [a] & David J. Cole [a]

[a] Department of Engineering , University of Cambridge , Trumpington Street, Cambridge , Cambridgeshire , CB2 1PZ , UK

Published online: 02 Apr 2012.

To cite this article: Julian P. Timings & David J. Cole (2012) Vehicle trajectory linearisation to enable efficient optimisation of the constant speed racing line, Vehicle System Dynamics: International Journal of Vehicle Mechanics and Mobility, 50:6, 883-901, DOI: 10.1080/00423114.2012.671946

To link to this article: http://dx.doi.org/10.1080/00423114.2012.671946

Vehicle System Dynamics
Vol. 50, No. 6, June 2012, 883–901

Taylor & Francis
Taylor & Francis Group

Vehicle trajectory linearisation to enable efficient optimisation of the constant speed racing line

Julian P. Timings and David J. Cole*

Department of Engineering, University of Cambridge, Trumpington Street, Cambridge, Cambridgeshire CB2 1PZ, UK

(*Received 20 January 2011; final version received 27 February 2012*)

A driver model is presented capable of optimising the trajectory of a simple dynamic nonlinear vehicle, at constant forward speed, so that progression along a predefined track is maximised as a function of time. In doing so, the model is able to continually operate a vehicle at its lateral-handling limit, maximising vehicle performance. The technique used forms a part of the solution to the motor racing objective of minimising lap time. A new approach of formulating the minimum lap time problem is motivated by the need for a more computationally efficient and robust tool-set for understanding on-the-limit driving behaviour. This has been achieved through set point-dependent linearisation of the vehicle model and coupling the vehicle–track system using an intrinsic coordinate description. Through this, the geometric vehicle trajectory had been linearised relative to the track reference, leading to new path optimisation algorithm which can be formed as a computationally efficient convex quadratic programming problem.

Keywords: motorsport; driver model; driver–vehicle system; model predictive control; nonlinear vehicle; lap time simulation

1. Introduction

Research into the driver–vehicle interface has been ongoing and remains a subject of much interest within the automotive field. In particular, a comprehensive understanding of this interaction is of considerable benefit to the motorsport industry. The research presented here focuses on enhancing our knowledge of driver–vehicle dynamics during limit-handling manoeuvres.

The task faced by a racing driver is to find the optimal balance of steer, brake and throttle controls that allows the car to traverse the circuit in the least amount of time. Two requirements need to be considered when searching for this optimum vehicle trajectory. The first requirement is to maximise the velocity of the vehicle at all points throughout the manoeuvre, limited by the available tyre force and maximum power produced by the engine. The second, potentially conflicting requirement, is to select a path so that, given the track boundaries, the total distance travelled is minimised. A compromise between these requirements is therefore sought which results in vehicle manoeuvre time being minimised. Previous research into this

*Corresponding author. Email: david.cole@eng.cam.ac.uk, djc1313@cam.ac.uk

ISSN 0042-3114 print/ISSN 1744-5159 online

http://dx.doi.org/10.1080/00423114.2012.671946
http://www.tandfonline.com

area can broadly be split into two categories of approach; path following such as that used by Thommyppillai *et al.* [1,2] and nonlinear optimisation with some form of track boundary constraint. The former, relies on the concept that the *optimum* racing line can be extracted from real-world telemetry data and by accurately tracking this pre-defined line while trying to maximise vehicle speed results in an optimum lap. By eliminating path generation from the problem Thommyppillai *et al.* are able to use Linear Optimal Preview Control Theory [3] to generate, off-line, a set of control schemes optimised for various dynamic equilibrium vehicle states. These are then employed by the driver depending on the vehicle operating condition. Such an approach has the advantage of being more amenable to computer solution; however, it could actually restrict maximising vehicle performance as it does not permit a driver to adjust their racing line depending on the vehicle's set-up. In contrast to this approach, by forming the lap time minimisation problem as one of nonlinear optimisation, it is possible to compute both the optimum path and speed trajectories online. Such methods have successfully been developed and applied by a number of researchers [4–7]. However, the fact that solving the required nonlinear optimisation problem is extremely computationally intensive and convergence to a solution is often not guaranteed, may explain the lack of published material detailing parametric studies.

Common to both types of approach are the inclusion of a number of human characteristics considered, to some extent, to represent the control behaviour of the human driver. These include: (i) preview information, designed to reflect the drivers ability see the road/track ahead and make anticipatory control decisions; (ii) adaptive control, to represent a drivers acute ability to adapt rapidly to varying plant dynamics or sudden alterations in operating conditions and (iii) an internal mental model of the vehicle dynamics used to estimate vehicle conditions at future points in time [8]. The research presented here uses these concepts and builds on the works of Keen and Cole [9] to develop a computationally efficient and robust technique for optimising the vehicle path over a course of finite width. In [10] the initial formulation of a constant speed path optimisation algorithm was presented with the driver model being formed as a time-varying model predictive control (MPC) controller. Focus here will be on the development of a refined algorithm and on improvements made in linearising the geometric positioning of the vehicle relative to the track. Attention will remain on optimum steering control at constant forward speed. The implications of this being a judicious choice of track geometry and vehicle speed in order for the optimisation problem to remain feasible, while still exercising limit-vehicle behaviour. Furthermore, the constant speed analysis means possible important vehicle dynamic characteristics such as combined-slip tyre operation and load transfer are not taken into account.

The next section starts by detailing the nonlinear vehicle model used for both the vehicle plant and internal human model. Next the various components that make up the driver model are outlined along with the formulation of the optimal control problem. This is followed by the derivation of the optimum path generation algorithm and the concept used to linearise the future vehicle trajectory which ultimately results in an efficient optimisation problem. The accuracy of the algorithm/method is then evaluated independently of the nonlinear vehicle, before the complete driver–vehicle system is brought together and a number of manoeuvre simulations performed.

2. Vehicle model

The model chosen to represent the lateral dynamics of the vehicle is the standard yaw/sideslip representation, often referred to as a *simple car model* or *bicycle model* [11]. An illustration of the vehicle model is given in Figure 1. The vehicle is assumed to have a steering system that

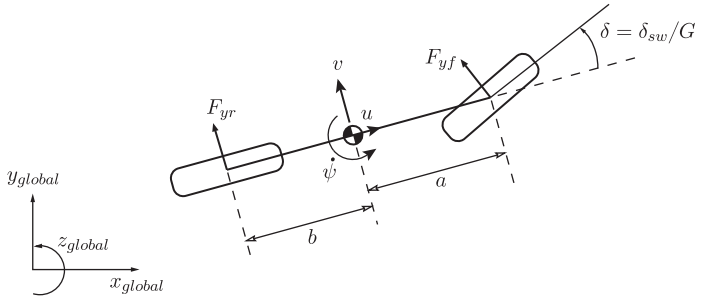

Figure 1. Single track vehicle model with associated forces and dimensions.

acts in such a way that a hand or steering wheel angle, δ_{sw}, results in a front road wheel angle, δ, through the steering ratio, G. Assuming small road wheel angles, the dynamic equations of motion for lateral velocity, v, and yaw rate, $\dot{\psi}$, read:

$$M_t(\dot{v} + u\dot{\psi}) = F_{yf} + F_{yr}, \tag{1}$$

$$I_z\ddot{\psi} = aF_{yf} - bF_{yr}. \tag{2}$$

The lateral tyre slip, α, is defined as the ratio of the lateral and longitudinal velocity of the tyre. Thus, for the front tyre it can be shown to be given by

$$\alpha_f = \frac{v + a\dot{\psi}}{u} - \frac{\delta_{\text{sw}}}{G} \tag{3}$$

and for the rear

$$\alpha_r = \frac{v - b\dot{\psi}}{u}. \tag{4}$$

The lateral tyre force characteristics are assumed to vary with α according to the well-known *Magic Formula* expression:

$$F_{yj} = -2D_j \sin\left(C_{yj} \arctan(B_{yj}\alpha_j - E_{yj}(B_{yj}\alpha_j - \arctan(B_{yj}\alpha_j)))\right). \tag{5}$$

The tyre nonlinearities are approximated using a linear-time-varying (LTV) model. By linearising the system at the current operating point, a local model which accurately represents the tyre dynamics within the neighbourhood of that operating point can be found. Choosing front and rear lateral slip as setpoint parameters allows the tyre characteristics to be linearised using a Taylor series expansion about each setpoint. Collecting only first-order terms enables the lateral force of the tyres to be described by the simple LTV expression:

$$F_{yj(t)} = C_{jy(t)}\alpha_{j(t)} + D_{jy(t)}, \tag{6}$$

where $C_{jy(t)}$ and $D_{jy(t)}$ denote the time-varying lateral slip stiffness and tyre force intercept at zero slip, respectively [9] (see Figure 2). Substituting the above force expressions along with slip equations (3), (4) into the vehicle equations of motion (1), (2) and rearranging, yields the

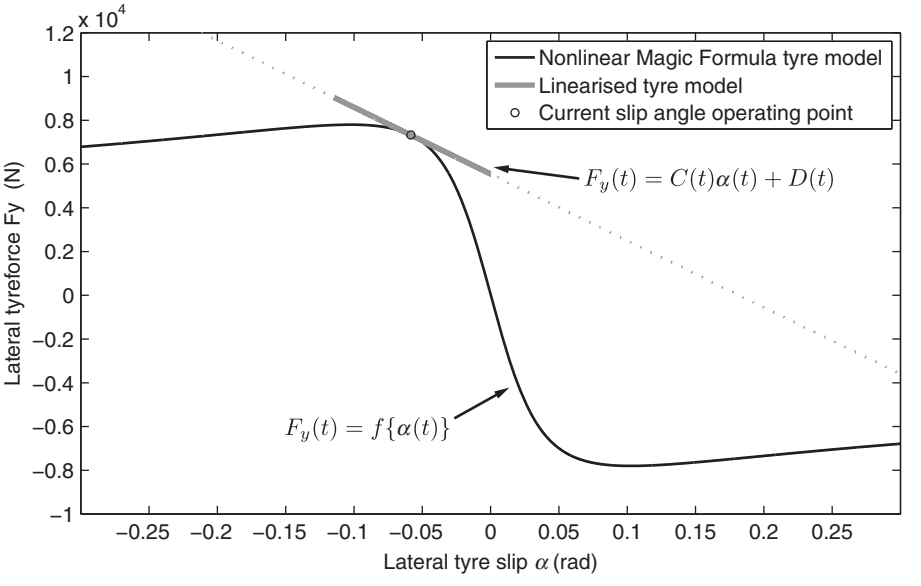

Figure 2. Linearisation of lateral tyre force about setpoint.

following LTV vehicle model

$$f_1 = \dot{v} = \frac{C_{fy} + C_{ry}}{M_t u} v + \frac{aC_{fy} - bC_{ry}}{M_t u} \dot{\psi} - u\dot{\psi} - \frac{C_{fy}\delta_{sw}}{M_t G} + \frac{D_{fy} + D_{ry}}{M_t}, \tag{7}$$

$$f_2 = \ddot{\psi} = \frac{aC_{fy} - bC_{ry}}{I_z u} v + \frac{a^2 C_{fy} + b^2 C_{ry}}{I_z u} \dot{\psi} - \frac{aC_{fy}\delta_{sw}}{I_z G} + \frac{aD_{fy} - bD_{ry}}{I_z}, \tag{8}$$

$$f_3 = \dot{\psi}. \tag{9}$$

Utilising the results of Pick and Cole [12], it is proposed that the vehicle model to be controlled comprises the vehicle dynamics coupled with the driver's bandwidth-limiting neuromuscular system (NMS) dynamics. The NMS can be represented as a second-order system acting on the steering wheel angle input to the vehicle, given by

$$\ddot{\delta}_{sw} + 2\zeta_n \omega_n \dot{\delta}_{sw} + \omega_n^2 \delta_{sw} = \omega_n^2 \delta_{\text{com}}, \tag{10}$$

where δ_{com} is the steering wheel angle commanded from the driver's brain and δ_{sw} now considered the output of the driver's NMS. ζ_{n} and ω_{n} denote the damping ratio and natural frequency of the NMS, respectively. The proposed NMS model demonstrates the characteristics of typical low-pass filter. It is, therefore, possible to add two additional equations to the vehicle model

$$f_4 = \ddot{\delta}_{sw} = -2\zeta_n \omega_n \dot{\delta}_{sw} - \omega_n^2 \delta_{sw} + \omega_n^2 \delta_{\text{com}}, \tag{11}$$

$$f_5 = \dot{\delta}_{sw}. \tag{12}$$

Coupling the NMS model and vehicle dynamics allows the system to be represented using the discrete time state-space description:

$$\boldsymbol{x}_{(k+1)} = \boldsymbol{A}_{(k)} \boldsymbol{x}_{(k)} + \boldsymbol{B}_{(k)} \Delta\delta_{\text{com}(k)} + \boldsymbol{E}_{(k)}, \tag{13}$$

$$\boldsymbol{z}_{(k)} = \boldsymbol{C}_{(k)} \boldsymbol{x}_{(k)}, \tag{14}$$

Table 1. Parameters, symbols and values for vehicle, tyres and driver's NMS.

Parameter	Symbol	Value
Vehicle mass	M_t	1050 kg
Vehicle yaw inertia	I_z	1500 kgm^2
CoG to front axle distance	a	0.92 m
CoG to rear axle distance	b	1.38 m
Steer to road wheel angle ratio	G	17
Stiffness factor (per tyre)	B_{yi}	17.5
Shape factor (per tyre)	C_{yi}	1.68
Peak factor (per tyre)	D_{yi}	3900 N
Curvature factor (per tyre)	E_{yi}	0.6
NMS damping ratio	ζ_n	0.7
NMS natural frequency	ω_n	18.9 rads^{-1}

where $\boldsymbol{E}_{(k)}$ contains the tyre force intercept terms from Equation (6) and the state vector is defined as

$$\boldsymbol{x}_{(k)} = [v_{(k)}\ \dot{\psi}_{(k)}\ \psi_{(k)}\ \dot{\delta}_{sw(k)}\ \delta_{sw(k)}\ \delta_{\mathrm{com}(k-1)}]^{\mathrm{T}}, \tag{15}$$

where the steering input command has been split into the sum of the steering command from the previous time step, now a system state, and the change in steering command during the present step.

The chassis, tyre and NMS parameter set used in the implementation of the vehicle system are given in Table 1.

3. Driver model

The driver model is formed as a model predictive controller. As detailed in Section 2, the vehicle to be controlled is nonlinear; furthermore, geometrically the objective of trying to minimise vehicle manoeuvre time subject to boundary constraints is also nonlinear. As demonstrated by Gerdts *et al.* [6], a solution can be found using nonlinear model predictive control (NMPC), combined with sequential quadratic programming (SQP). However, there is large computational cost associated by overcoming the non-convexity of the problem, together with uncertainty regarding its convergence. An alternative MPC formulation is presented by Maciejowski [13], whereby if the internal model of the plant is linear and the constraints imposed as linear inequalities, the constrained MPC problem can be formed as a convex quadratic programming (QP) problem. In comparison to SQP, which linearises the constraints implicitly, Maciejowski's approach requires the solution of a single QP problem each time step, as opposed to the numerous QP sub-problems being solved sequentially in SQP in order to establish a suitable search direction towards an optimum. Furthermore, the convexity of the solution space in QP guarantees termination of the optimisation problem, avoiding the problems associated with the multiple local minima that arise in nonlinear optimisation. Therefore, the objective here is to formulate the problem in such a way that this more efficient and reliable MPC framework can be adopted.

3.1. *Preview and predicted vehicle trajectory*

A key concept of predictive control is the idea of a receding horizon, allowing information about the desired future trajectory to be gathered and using this as the basis for control

decisions. Such a strategy is analogous to a real driver's line of sight and their ability to assess the path ahead and make steering (and brake/throttle) decisions accordingly. An essential part of this is the internal model of the plant used to produce a future predicted response of the vehicle at each iteration. Here, the internal model is taken to be the LTV vehicle model developed in Section 2. Furthermore, in order to determine the future vehicle position, the *variable-model-preview* concept detailed by Keen [14] is adopted. Many of the driver controllers presented in the literature [1,15,16] fix the internal/prediction model and control input over the horizon and iterate these to estimate the future state and output trajectories, $\hat{\boldsymbol{x}}_{(k+i)}$ and $\hat{\boldsymbol{z}}_{(k+i)}$, respectively. However, Keen and Cole determined that a more accurate estimation of the vehicle's future states can be obtained by using the discarded input commands from the previous control cycle (time step $k-1$). Iterating (13), open-loop, with the series of delta input commands, $\Delta\hat{\delta}_{\text{com}(k+i|k-1)}$ for $i = 1 \ldots N_p - 1$, enables an estimation of the predicted trajectory for the next control cycle to be found. Since (13) and (14) are time varying in nature, the prediction results in a sequence of linearised vehicle models that approximate the future dynamics of the vehicle along the horizon. This future knowledge of the expected vehicle dynamics enhances the prediction strategy and is an essential part of the control strategy.

The track centreline is taken as the reference trajectory on which all preview information is based. Figure 3 sets out the reference trajectory parameters and how they relate to the previous predicted vehicle trajectory. As shown, the track centreline is defined in the global reference frame using an intrinsic coordinate description $(\mathrm{d}s_r, \phi_r)$. The exact points which make up the track centreline description are those coincident with lines normal to the centreline that also pass through the predicted positions of the vehicle, as illustrated. This then allows the lateral displacement and heading angle errors $\hat{y}_{\text{err}(k+i|k-1)}$ and $\hat{\phi}_{\text{err}(k+i|k-1)}$, respectively, to be calculated and stored.

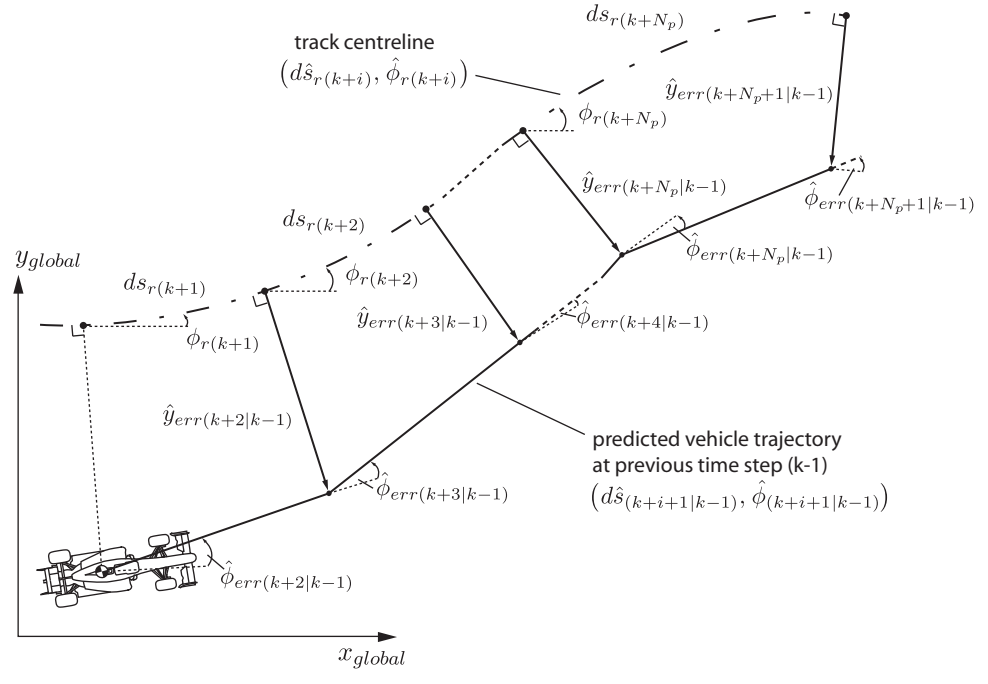

Figure 3. Predicted vehicle trajectory and corresponding reference trajectory parameters.

3.2. *Predictive control formulation*

At this stage, the track reference trajectory and linearised vehicle dynamics within the predicted trajectory are uncoupled. The following quadratic cost function is therefore proposed to connect the two

$$J_{(k)} = \sum_{i=1}^{N_p} \hat{\boldsymbol{z}}^{\mathrm{T}}_{(k+i)} \boldsymbol{Q}_{1(k+i)} \hat{\boldsymbol{z}}_{(k+i)} + R_{(k+i)} \Delta \hat{\delta}^2_{\mathrm{com}(k+i-1)} + \boldsymbol{Q}^{\mathrm{T}}_{2(k+i)} \hat{\boldsymbol{z}}_{(k+i)}, \tag{16}$$

where $\boldsymbol{Q}_{1(k+i)}$ and $\boldsymbol{Q}_{2(k+i)}$ are semi-positive-definite diagonal matrices which contain the weights of relative importance placed on the output objectives which later are also used to incorporate reference trajectory information. The positive-definite scalar, $R_{(k+i)}$, determines the extent to which the change in commanded steering demand, $\Delta\hat{\delta}_{\mathrm{com}}$, contributes to the minimisation of the cost function. Substituting the linearised state-space output equation (14) into (16) leads to

$$\begin{aligned} J_{(k)} = \sum_{i=1}^{N_p} & \hat{\boldsymbol{x}}^{\mathrm{T}}_{(k+i)} \hat{\boldsymbol{C}}^{\mathrm{T}}_{(k+i)} \boldsymbol{Q}_{1(k+i)} \hat{\boldsymbol{C}}_{(k+i)} \hat{\boldsymbol{x}}_{(k+i)} + R_{(k+i)} \Delta \hat{\delta}^2_{\mathrm{com}(k+i-1)} \\ & + \boldsymbol{Q}^{\mathrm{T}}_{2(k+i)} \hat{\boldsymbol{C}}_{(k+i)} \hat{\boldsymbol{x}}_{(k+i)}. \end{aligned} \tag{17}$$

Writing in a more compact form yields

$$\begin{aligned} J_{(k)} = \sum_{i=1}^{N_p} & \begin{bmatrix} \Delta\hat{\delta}_{\mathrm{com}(k+i-1)} \\ \hat{\boldsymbol{x}}_{(k+i)} \end{bmatrix}^{\mathrm{T}} \begin{bmatrix} R_{(k+i)} & 0 \\ 0 & \hat{\boldsymbol{C}}^{\mathrm{T}}_{(k+i)} \boldsymbol{Q}_{1(k+i)} \hat{\boldsymbol{C}}_{(k+i)} \end{bmatrix} \begin{bmatrix} \Delta\hat{\delta}_{\mathrm{com}(k+i-1)} \\ \hat{\boldsymbol{x}}_{(k+i)} \end{bmatrix} \\ & + \begin{bmatrix} 0 \\ \boldsymbol{Q}^{\mathrm{T}}_{2(k+i)} \hat{\boldsymbol{C}}_{(k+i)} \end{bmatrix}^{\mathrm{T}} \begin{bmatrix} \Delta\hat{\delta}_{\mathrm{com}(k+i-1)} \\ \hat{\boldsymbol{x}}_{(k+i)} \end{bmatrix}, \end{aligned} \tag{18}$$

a finite-dimensional convex quadratic program (QP). A common formulation involves eliminating the future predicted state variables and recasting the problem in terms of the current state of the system and its optimal input profile. Such an approach results in a quadratic function whose Hessian, $H_{(k)}$, is dense with dimensions which grow linearly with N_p. According to [17,18], this results in the time required to minimise the quadratic cost growing cubically with N_p, with $O(N_p^3(n+m)^3)$ being the operations required per step for a problem with n states and m input variables. An alternative MPC formulation, however, retains the states as explicit variables within the optimisation problem while employing the model equation as an *equality* constraint. Matrix dimensions continue to grow linearly with N_p; however, the resultant matrix has a banded structure with the nonzero entries lying on or close to the principal diagonal. Since the bandwidth of the matrix is now independent of N_p, the cost of optimisation grows linearly as opposed to cubically with N_p, thus $O(N_p(n+m)^3)$. With the use of long prediction/control horizons motivated from both a closed-loop stability standpoint [13] and in order to replicate the depth of vision of a human driver, the banded structured MPC formulation is adopted here. Thus, the following model equation constraint is imposed

$$\hat{\boldsymbol{x}}_{(k+i+1)} = \hat{\boldsymbol{A}}_{(k+i)} \hat{\boldsymbol{x}}_{(k+i)} + \hat{\boldsymbol{B}}_{(k+i)} \Delta\hat{\delta}_{\mathrm{com}(k+i)} + \hat{\boldsymbol{E}}_{(k+i)}, \tag{19}$$

for $i = 0 \ldots N_p - 1$. Equations (18) and (19) can now be written in the framework of a general QP problem with the possibility of *inequality* constraints on the predicted input and output

trajectories.

$$\min_{\theta_{(k)}} J_{(k)} = \tfrac{1}{2}\theta_{(k)}^{\mathrm{T}} H_{(k)} \theta_{(k)} + \eta_{(k)}^{\mathrm{T}} \theta_{(k)} \quad (H_{(k)} = H_{(k)}^{\mathrm{T}} \geq 0) \tag{20}$$

subject to

$$\Gamma_{(k)} \theta_{(k)} = \gamma_{(k)} \tag{21}$$

and

$$\Omega_{(k)} \theta_{(k)} \leq \omega_{(k)} \tag{22}$$

where

$$\theta_{(k)} = \begin{bmatrix} \Delta\hat{\delta}_{\mathrm{com}(k)} \\ \hat{\boldsymbol{x}}_{(k+1)} \\ \Delta\hat{\delta}_{\mathrm{com}(k+1)} \\ \hat{\boldsymbol{x}}_{(k+2)} \\ \vdots \\ \Delta\hat{\delta}_{\mathrm{com}(k+N_p-1)} \\ \hat{\boldsymbol{x}}_{(k+N_p)} \end{bmatrix}, \quad \eta_{(k)} = \begin{bmatrix} 0 \\ \hat{\boldsymbol{C}}_{(k+1)}^{\mathrm{T}} \boldsymbol{Q}_{2(k+1)} \\ \vdots \\ 0 \\ \hat{\boldsymbol{C}}_{(k+N_p)}^{\mathrm{T}} \boldsymbol{Q}_{2(k+N_p)} \end{bmatrix},$$

$$H_{(k)} = 2 \begin{bmatrix} R_{(k+1)} & 0 & \cdots & 0 & 0 \\ 0 & \hat{\boldsymbol{C}}_{(k+1)}^{\mathrm{T}} \boldsymbol{Q}_{1(k+1)} \hat{\boldsymbol{C}}_{(k+1)} & \cdots & 0 & 0 \\ \vdots & \vdots & \ddots & \vdots & \vdots \\ 0 & 0 & \cdots & R_{(k+N_p)} & 0 \\ 0 & 0 & \cdots & 0 & \hat{\boldsymbol{C}}_{(k+N_p)}^{\mathrm{T}} \boldsymbol{Q}_{1(k+N_p)} \hat{\boldsymbol{C}}_{(k+N_p)} \end{bmatrix}$$

and

$$\Gamma_{(k)} = \begin{bmatrix} -\hat{\boldsymbol{B}}_{(k)} & \boldsymbol{I} & 0 & 0 & \cdots & 0 & 0 & 0 \\ 0 & -\hat{\boldsymbol{A}}_{(k+1)} & -\hat{\boldsymbol{B}}_{(k+1)} & \boldsymbol{I} & \cdots & 0 & 0 & 0 \\ \vdots & \vdots & \vdots & \vdots & \ddots & \vdots & \vdots & \vdots \\ 0 & 0 & 0 & 0 & \cdots & -\hat{\boldsymbol{A}}_{(k+N_p-1)} & -\hat{\boldsymbol{B}}_{(k+N_p-1)} & \boldsymbol{I} \end{bmatrix},$$

$$\gamma_{(k)} = \begin{bmatrix} \hat{\boldsymbol{A}}_{(k)} \boldsymbol{x}_{(k)} + \hat{\boldsymbol{E}}_{(k)} \\ \hat{\boldsymbol{E}}_{(k+1)} \\ \vdots \\ \hat{\boldsymbol{E}}_{(k+N_p-1)} \end{bmatrix}$$

and

$$\Omega_{(k)} = \begin{bmatrix} 0 & \hat{\boldsymbol{C}}_{(k+1)} & \cdots & 0 & 0 \\ 0 & -\hat{\boldsymbol{C}}_{(k+1)} & \cdots & 0 & 0 \\ \vdots & \vdots & \ddots & \vdots & \vdots \\ 0 & 0 & \cdots & 0 & \hat{\boldsymbol{C}}_{(k+N_p)} \\ 0 & 0 & \cdots & 0 & -\hat{\boldsymbol{C}}_{(k+N_p)} \end{bmatrix}, \quad \omega_{(k)} = \begin{bmatrix} z_{\mathrm{upper}(k+1)} \\ z_{\mathrm{lower}(k+1)} \\ \vdots \\ z_{\mathrm{upper}(k+N_p)} \\ z_{\mathrm{lower}(k+N_p)} \end{bmatrix}.$$

In the formulation above, inequality constraints are only placed on the output variables, $\hat{z}_{(k+i)}$ (and not on the change in commanded steer $\Delta\hat{\delta}_{\mathrm{com}(k+i)}$) with the z_{upper} and z_{lower} vectors representing the corresponding upper and lower bounds, respectively.

3.3. *Path optimisation algorithm*

As noted earlier, in order to minimise vehicle manoeuvre times it is necessary to maximise the velocity of the vehicle while simultaneously trying to minimise the total distance travelled to complete the manoeuvre. Casanova [4] achieved this using a nonlinear time-to-distance transformation scalar which formed the basis of the cost function. Here, the aim is to avoid a nonlinear cost function and therefore the need to resort to nonlinear optimisation techniques. However, to enable use of the efficient MPC framework developed thus far, it is necessary that the cost function remains quadratic in linearly defined outputs. To achieve this a number of approximations are introduced, the consequences of which are evaluated in a subsequent section. It is posed that an alternative way of minimising manoeuvre time is to maximise the total distance travelled in a fixed amount of time [6,19]. With the velocity of the vehicle considered constant, a path optimisation algorithm is sought which attempts to establish the path of least distance. Figure 4 introduces the concept of describing the future predicted position of the vehicle relative to the track using an intrinsic coordinate description, that is, in terms the incremental distance travelled by the vehicle in one time step $\mathrm{d}s = VT \approx uT$ and the direction of the vehicle's velocity vector $\phi = \beta + \psi$. The objective is to find the corresponding description of the track centreline in relation to the vehicle trajectory and optimise this, such that the incremental distance travelled along the track centreline $\mathrm{d}s_r$ is maximised in a fixed amount of time. Therefore, from Figure 4 we can obtain

$$\mathrm{d}s_r = r_r \,\mathrm{d}\phi_r, \tag{23}$$

$$\mathrm{d}n = (r_r - y_{\mathrm{err}})\,\mathrm{d}\phi_r. \tag{24}$$

Substituting, (23) into (24), therefore, leads to

$$\mathrm{d}n = \mathrm{d}s_r - y_{\mathrm{err}}\,\mathrm{d}\phi_r. \tag{25}$$

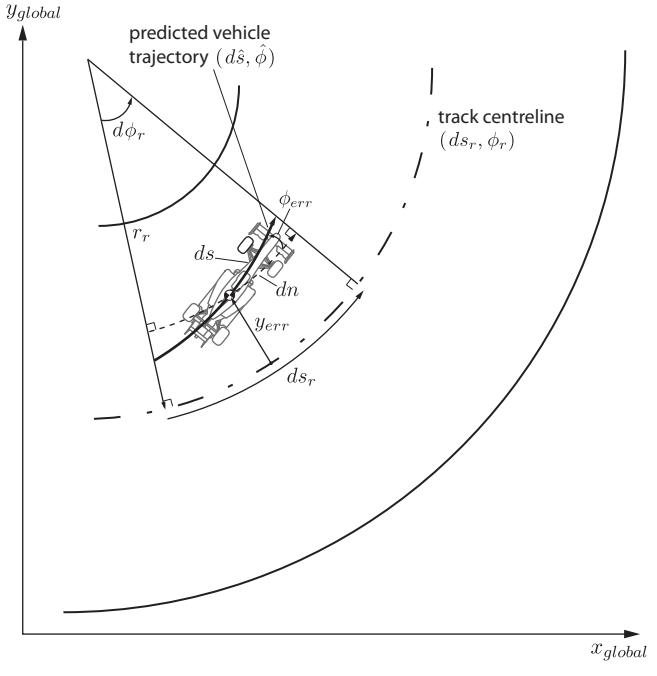

Figure 4. Geometric definitions for derivation of intrinsic vehicle–track progression expression.

Furthermore,

$$\begin{aligned} \mathrm{d}n &= \mathrm{d}s \cos \phi_{\mathrm{err}} \\ &\approx \mathrm{d}s \left(1 - \frac{\phi_{\mathrm{err}}^2}{2}\right), \end{aligned} \tag{26}$$

taking only the first two terms of a power series expansion of cos. Equating (25) and (26) and rearranging yield the distance travelled along the track centerline in one time step

$$\mathrm{d}s_r = \mathrm{d}s + y_{\mathrm{err}}\, \mathrm{d}\phi_r - \mathrm{d}s \frac{\phi_{\mathrm{err}}^2}{2}. \tag{27}$$

This expression is valid provided ϕ_{err} remains within the bounds in which the approximation of cos remains valid. Summating expression (27) from $i = 1 \ldots N_p$ yields the nominal distance travelled along the track centreline over the prediction horizon

$$\sum_{i=1}^{N_p} \mathrm{d}s_{r(k+i)} = \sum_{i=1}^{N_p} \mathrm{d}s + \hat{y}_{\mathrm{err}(k+i)}\, \mathrm{d}\phi_{r(k+i)} - \mathrm{d}s \frac{\hat{\phi}_{\mathrm{err}(k+i)}^2}{2}. \tag{28}$$

By maximising (28), the progress of the vehicle along the track in a fixed time interval (N_pT) is maximised. Note that for the constant forward speed case $\mathrm{d}s$ has no time-dependence, allowing the first term of (28) to be excluded from any cost function. Furthermore, in order for the function to be maximised using a solver which seeks minima, the sign of each term should be reversed. In line with these two points, the following candidate quadratic cost function is proposed, where the weights q and R are no longer time dependent

$$J_{(k)} = \sum_{i=1}^{N_p} q \left(-\hat{y}_{\mathrm{err}(k+i)}\, \mathrm{d}\phi_{r(k+i)} + \mathrm{d}s \frac{\hat{\phi}_{\mathrm{err}(k+i)}^2}{2} \right) + R \Delta \hat{\delta}_{\mathrm{com}(k+i-1)}^2. \tag{29}$$

3.4. *Linearising lateral displacement and heading angle errors*

A key requirement for the optimisation problem to remain a convex QP problem is that the terms which make up (29) can be linearly reproduced from the system states and inputs, as state-space outputs. The reference trajectory terms associated with the track geometry, $\mathrm{d}\phi_r$ and r_r, can be approximated along the horizon using the information gained from plotting the previous optimised predicted trajectory, thus $r_{r(k+i)} \approx r_{r(k+i+1|k-1)}$ and $\mathrm{d}\phi_{r(k+i)} \approx \mathrm{d}\phi_{r(k+i+1|k-1)}$. Furthermore, the heading error between the vehicle and track, $\hat{\phi}_{\mathrm{err}}$, assumed to be the difference in angle between the velocity vector of the vehicle and track centreline can be defined as

$$\begin{aligned} \hat{\phi}_{\mathrm{err}(k+i)} &= (\hat{\beta}_{(k+i)} + \hat{\psi}_{(k+i)}) - \phi_{r(k+i)} \\ &\approx (\hat{\beta}_{(k+i)} + \hat{\psi}_{(k+i)}) - \phi_{r(k+i+1|k-1)}, \end{aligned} \tag{30}$$

for $i = 1 \ldots N_p$, where the body side slip angle is approximated as $\beta \approx v/u$.

The perpendicular distance between the vehicle and track centreline, $\hat{y}_{\mathrm{err}}$, is a nonlinear function of the system states and cannot straightforwardly be made an output of the system. A method is needed to linearise $\hat{y}_{\mathrm{err}}$ and therefore preserve a linear positioning of the vehicle relative to the track. The idea is therefore introduced that two consecutive optimisations produce very similar predicted trajectories. Primarily, the only difference between the two arises from the one time step of extra information that has entered the problem at the end of the horizon

along with that lost information at the beginning of the horizon as it recedes. On this basis, it is proposed that $\hat{y}_{\text{err}}$ can be approximated using

$$\hat{y}_{\text{err}(k+i)} = \hat{y}_{\text{err}(k+i+1|k-1)} + \Delta\hat{y}_{\text{err}(k+i)}. \tag{31}$$

That is to say, a summation of the lateral displacement error from the previous prediction, now effectively a constant, and the change in lateral displacement of the vehicle relative to the track centreline between two consecutive predicted paths. Hence, it is now only necessary to derive a linear expression which describes the variation of the later term, $\Delta\hat{y}_{\text{err}(k+i)}$. With the forward speed of the vehicle assumed constant, any lateral position change must be a result of the heading direction of the vehicle changing along the horizon. Figure 5 sets out the connection between two consecutive vehicle paths when an intrinsic coordinate description is used. From Figure 5 it is possible to derive the following expression for how the change in lateral position of the vehicle evolves along the horizon as a linear function of the new heading direction of the vehicle body, $\hat{\phi}_{(k+i)}$.

$$\hat{\delta}_{y(k+i)} = \hat{\delta}_{y(k+i-1)} \cos(\hat{\phi}_{(k+i+1|k-1)} - \hat{\phi}_{(k+i|k-1)}) + \mathrm{d}s(\hat{\phi}_{(k+i)} - \hat{\phi}_{(k+i+1|k-1)}). \tag{32}$$

There is also a correspondingly small change longitudinal displacement which, depending on the relative orientation of vehicle to track, can further contribute to $\Delta\hat{y}_{\text{err}(k+i)}$. From Figure 5, this can be approximated using

$$\begin{aligned}\hat{\delta}_{x(k+i)} = {} & \hat{\delta}_{x(k+i-1)} \cos(\hat{\phi}_{(k+i+1|k-1)} - \hat{\phi}_{(k+i|k-1)}) \\ & + \hat{\delta}_{y(k+i-1)} \sin(\hat{\phi}_{(k+i+1|k-1)} - \hat{\phi}_{(k+i|k-1)}).\end{aligned} \tag{33}$$

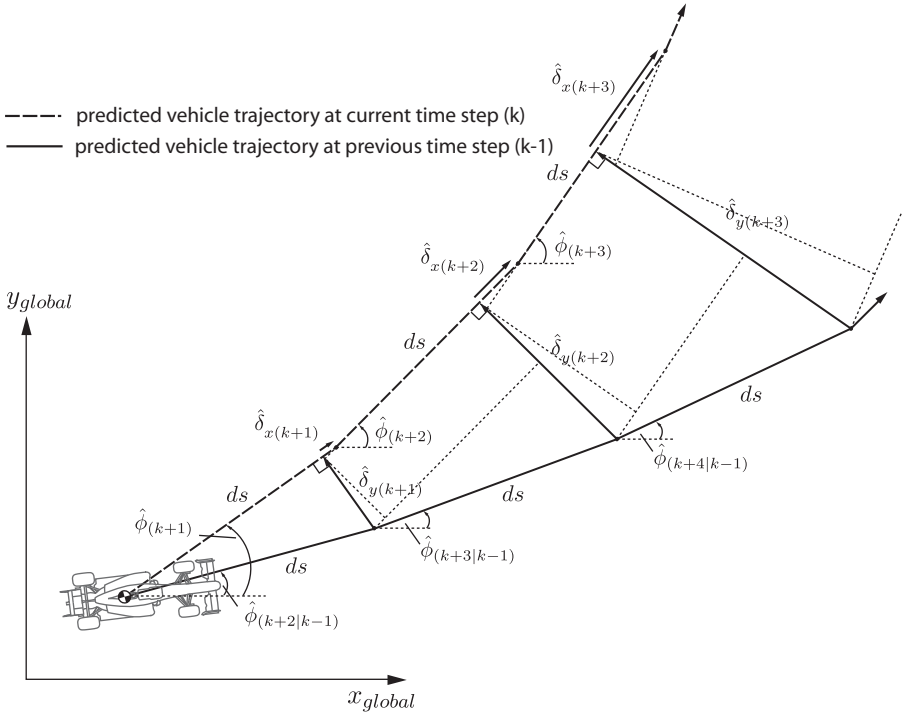

Figure 5. Initial geometric definitions for derivation of intrinsic displacement error expressions, due to a change in heading angle, for two consecutive predicted vehicle paths.

Figure 6 illustrates how these changes of vehicle displacement along the horizon relate to the new position of the vehicle relative to the track centreline reference. The figure somewhat exaggerates the change in the heading direction of the vehicle between two consecutive trajectories in order to highlight the approximations made. Thus, the terms $\hat{\delta}_{x(k+i)}$ and $\hat{\delta}_{y(k+i)}$ are used to approximate $\Delta\hat{y}_{\mathrm{err}(k+i)}$ by resolving each in a direction perpendicular to the track centreline based on the previous predicted heading angle errors. Hence,

$$\Delta\hat{y}_{\mathrm{err}(k+i)} \approx \hat{\delta}_{y(k+i)} \cos(\hat{\phi}_{\mathrm{err}(k+i+1|k-1)}) + \hat{\delta}_{x(k+i)} \sin(\hat{\phi}_{\mathrm{err}(k+i+1|k-1)}) \tag{34}$$

for $i = 1 \ldots N_p$. By incorporating $\hat{\delta}_{y(k+i-1)}$ and $\hat{\delta}_{x(k+i-1)}$ as states within the MPC model equation and through appropriate augmentation of the state-space matrices $\boldsymbol{A}$ and $\boldsymbol{C}$, enables $\Delta\hat{y}_{\mathrm{err}(k+i)}$ to be made an output of the system. Equation (31) can then be reproduced within the cost function and optimised, along with $\hat{\phi}_{\mathrm{err}(k+i)}$, over the horizon so as to maximise the progression of the vehicle along the track.

3.5. *Track boundary and tyre slip constraints*

The fundamental restriction on minimum time manoeuvring is that imposed by the track boundaries. This is commonly observed in real-life motor racing as drivers are often seen 'shorting' the track at every opportunity to gain fractions of a second over their competitors. From a modelling standpoint, the track boundaries are implemented as constraints on the states/outputs, bounding the permissable position of the vehicle relative to the track centreline. Having linearised this relationship in a novel way, this can be achieved straightforwardly by

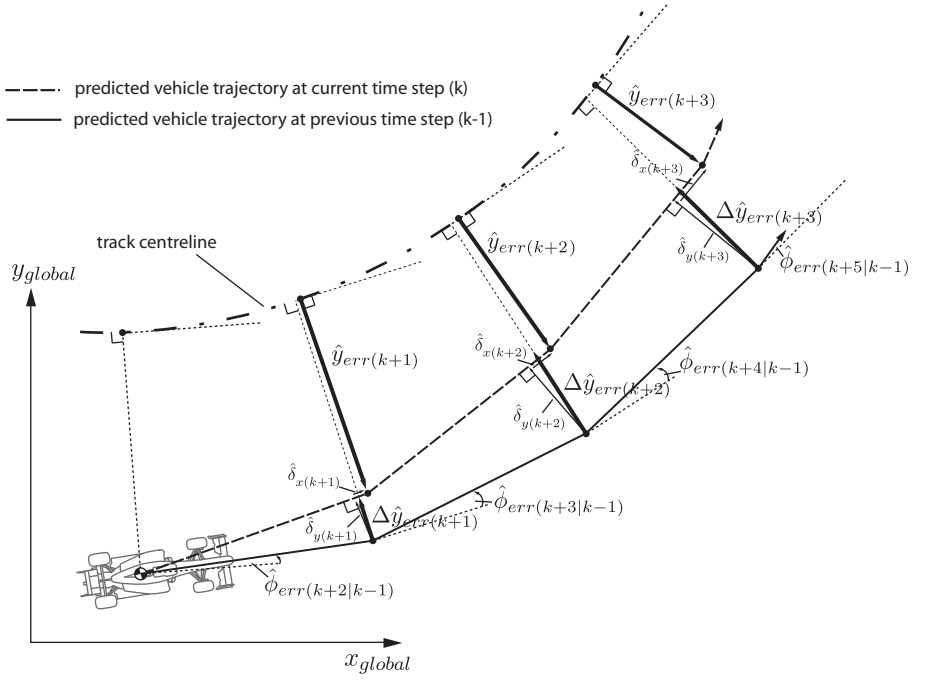

Figure 6. Approximation of $y_{\mathrm{err}(k+i)}$ using the change in lateral displacement between successive predicted vehicle path trajectories $\Delta y_{\mathrm{err}(k+i)}$, which in turn is determined using $\hat{\delta}_{x(k+i)}$ and $\hat{\delta}_{y(k+i)}$.

ensuring

$$\pm\hat{y}_{\mathrm{err}(k+i)} \leq \frac{w_r}{2} - w \tag{35}$$

for $i = 1 \ldots N_p$, where w_r is the width of the track and w is the half-track-width of the vehicle. In addition to the boundary constraints, tyre lateral slips α_f and α_r are constrained to ensure that the tyres operate only within the positive slope region of the tyre force curves, restricting the tyres operating beyond their saturation limit where it is unlikely optimum performance will be found. Hence, the lateral slip limit α_{bound} is set to the point at which maximum lateral tyre force occurs

$$\pm\hat{\alpha}_{j(k+i)} \leq \alpha_{\mathrm{bound}}, \tag{36}$$

for $i = 1 \ldots N_p$. The linear nature of constraint equations (35) and (36) allows them to be easily incorporated into the optimisation problem through inequality (22).

In summary, the sequence of operations on which the driver model is based is as follows. For a given control cycle, the controller measures the vehicle states in full and predicts the future vehicle state trajectories based on the previous cycle's assumed future input steering changes, $\Delta\hat{\delta}_{\mathrm{com}(k+i|k-1)}$. These state trajectories are used to plot an estimate of the future coordinate position of the vehicle on the track, allowing both information about the track ahead to be gathered and the positioning of the vehicle relative to the track centreline. The MPC problem is next formulated as per Section 3.2 and used to minimise the vehicle manoeuvre time cost function (29), subject to the track boundary and tyre lateral slip constraints (35) and (36), to produce the new optimal control vector, $\Delta\hat{\delta}_{\mathrm{com}(k+i|k)}$. The first element of this vector is combined with the previous steer input, such that $\delta_{\mathrm{com}(k)} = \delta_{\mathrm{com}(k-1)} + \Delta\hat{\delta}_{\mathrm{com}(k)}$, which is applied to the vehicle. The remaining elements are the assumed future input steering changes for the next cycle allowing a new set of prediction matrices to be formed and the sequence repeated.

4. Testing optimum path algorithm approximations

As detailed in Section 3.3, in order for the cost function to remain quadratic in linearly defined system outputs, the key approximation made during the derivation of the path optimisation algorithm was that $\cos(\phi_{\mathrm{err}})$ can be approximated using the first two terms of the power series expansion. To evaluate this and therefore how well the cost function acts to maximise the distance travelled along the track centreline in a fixed amount of time, the nonlinear vehicle model is replaced with a very simple massless point model (Figure 7). The model travels at a constant forward velocity u and is free to yaw according to the dynamic expression

$$\dot{\psi} = \delta_{\mathrm{sw}}, \tag{37}$$

where δ_{sw} is the system input and will continue to be referred to as the steering wheel angle for convenience. Furthermore, two simulations are set up using a double 90° s-bend track of finite width. Since the vehicle will have to negotiate a coupled left and right bend, large angular deviations from the track centreline are likely to occur in the transition phase between the two corners. To exaggerate the angular deviation further, in the first simulation (Figure 8(a)) the track width is made comparable to the corner radii so as to encourage 'straight-lining' of the manoeuvre. Overlaid on the figure is also the 'optimum path' or route of least distance, generated analytically by determining the tangent line connecting the inner radii of each corner. Figure 8(b) illustrates the results of a repeat simulation using a narrower track width

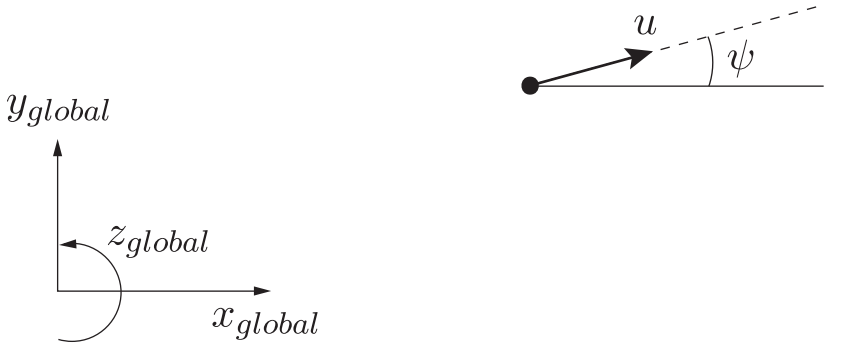

Figure 7. Massless point vehicle model used for evaluation of path optimisation cost function.

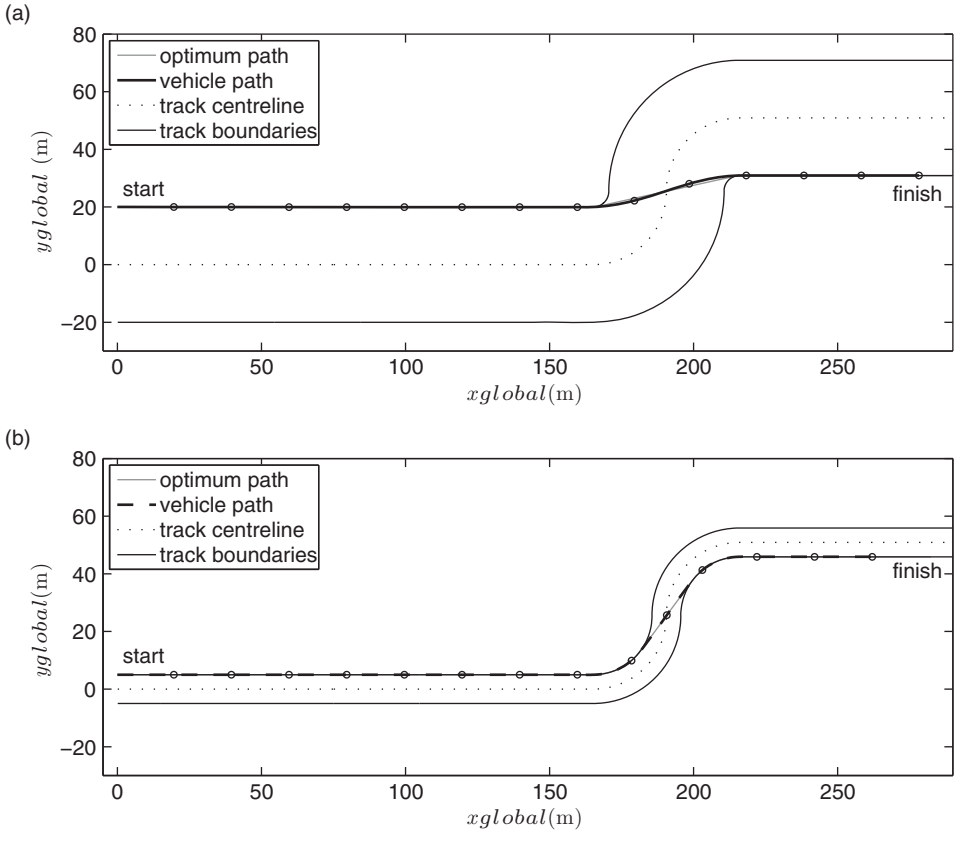

Figure 8. Optimised vehicle path simulation results, with marked 1 s intervals, for extreme s-bend manoeuvre using massless point model travelling at 20 m/s. Overlaid with path of least distance derived analytically. A road width of 40 m is used in simulation (a) and 10 m during simulation (b).

which generates reduced heading angle error between vehicle and track centreline paths. The simulation and control parameters used during these tests are given in Table 2.

By eliminating the vehicle dynamics and tyre limitations, the driver model is able to generate a trajectory very similar to the geometric path of least distance. However, the vehicle path is not perfect. To examine this deviation further, Figure 9 shows the displacement error between the optimum and actual vehicle path generated by the driver model as a function of the

Table 2. Simulation and constraint parameters used during the path optimisation algorithm testing.

Parameter	Symbol	Value
Discrete time step	T	0.02 s
Preview horizon	N_p	400
Maximise distance travelled weight	q	10
$\Delta\delta_{sw}$ effort weight	R	1
Vehicle forward speed	u	20 m/s

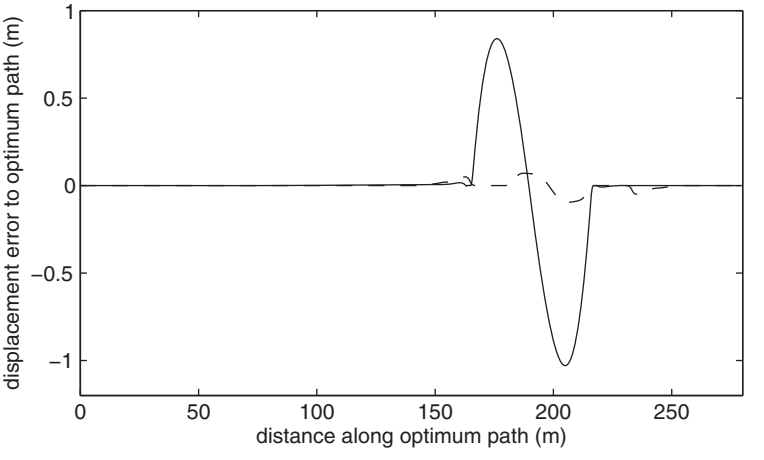

Figure 9. Displacement error between vehicle and optimum path as a function of distance travelled along each optimum path, corresponding to Figure 8(a) (solid) and Figure 8(b) (dashed).

distance travelled along each of the two optimum paths. As can be seen, during the wide track simulation, the significant time spent at very large angular deviations ($\phi_{\text{err}} \approx 1.1$ rad) results in a maximum displacement error of approximately 1 m. However, reducing the track width and thus peak angular deviation to $\phi_{\text{err}} \approx 0.7$ rad, reduces the displacement error to the desired path by more than an order of magnitude to <0.1 m. These results highlight the limitations of the method in terms of geometric severity of the track. Nonetheless, if the extra distance travelled along the track is calculated by comparing the actual vehicle path to the optimum, the optimum path is 0.19 m 'ahead' by the end of the wide track simulation and only 0.007 m in front by the end of the narrower road width simulation. These results demonstrate that during typical manoeuvre scenarios, the path generated by the algorithm is sufficiently close to the optimum path.

5. Path optimised simulations

To demonstrate the performance of the complete steering controller, the nonlinear vehicle model detailed in Section 2 is reintroduced and similar s-bend simulations are performed. The vehicle forward speed is set to 30 m/s so that the steering controller will have to make full use of the circuit width and vehicle operating limits. The other simulation and control parameters are given in Table 3. The vehicle path and parameter time histories are shown in Figures 10 and 11 respectively. As can be seen from Figure 10, shortly after the start of the simulation the controller begins to steer the vehicle towards the outside of the track in anticipation of

Table 3. Simulation and constraint parameters used during the path optimisation simulations using the nonlinear vehicle model.

Parameter	Symbol	Value
Discrete time step	T	0.02 s
Maximise distance travelled weight	q	10
$\Delta\delta_{\text{com}}$ effort weight	R	1
Track/road width	w_r	10 m
Vehicle half track	w	0 m
Side-slip constraint	α_{bound}	0.09
Vehicle forward speed	u	30 m/s

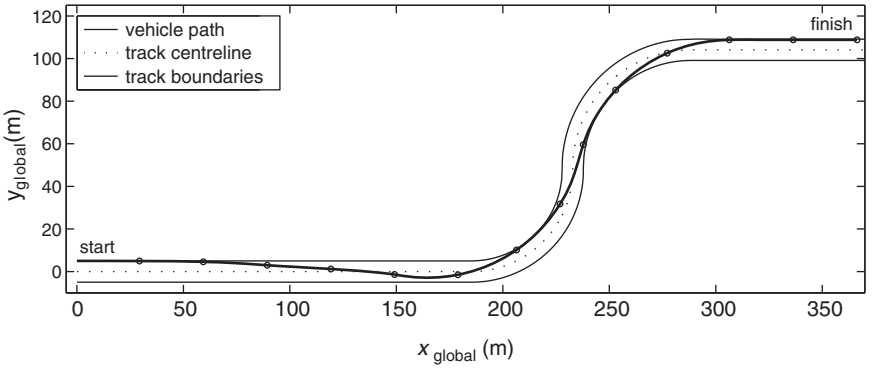

Figure 10. Path optimised simulation results for s-bend manoeuvre at 30 m/s with marked 1 s intervals using a preview horizon $N_p = 300$.

the approaching corner sequence. The controller stops short of driving the vehicle to the very edge of the circuit as the future predicted trajectories have enabled the controller to establish that it can navigate the upcoming bend(s) with an early turn-in and still operate within the tyre limits. The set-up parameters chosen mean the vehicle is front axle limited, the time histories of Figure 11 demonstrate how the controller ensures the vehicle continually operates at the front side-slip angle corresponding to max lateral tyre force.

The results of another simulation are shown in Figures 12 and 13. The horizon N_p has been increased to 500 steps to provide further preview of the manoeuvre. Again the driver model makes full use of the track width and continually operates the vehicle at its handling limit in order to maximise the distance the vehicle travels during the simulation. Regarding the choice of horizon, unlike the works of Thommyppillai *et al.* [1], which through the identification of diminishing preview gains allows the so-called 'full-preview' to be established, no formal method has been used here to select the horizon length. Ultimately, the horizon should be established through a trade-off of computational time and optimality with regards to the nonlinear solution.

6. Conclusions

The research detailed is concerned with the development of a mathematical model of a human racing driver. It seeks to build on previous works demonstrating how MPC theory and the 'internal model' concept from human neuroscience form a good strategy for modelling driver behaviour. A new approach of formulating the minimum manoeuvre time problem has, in

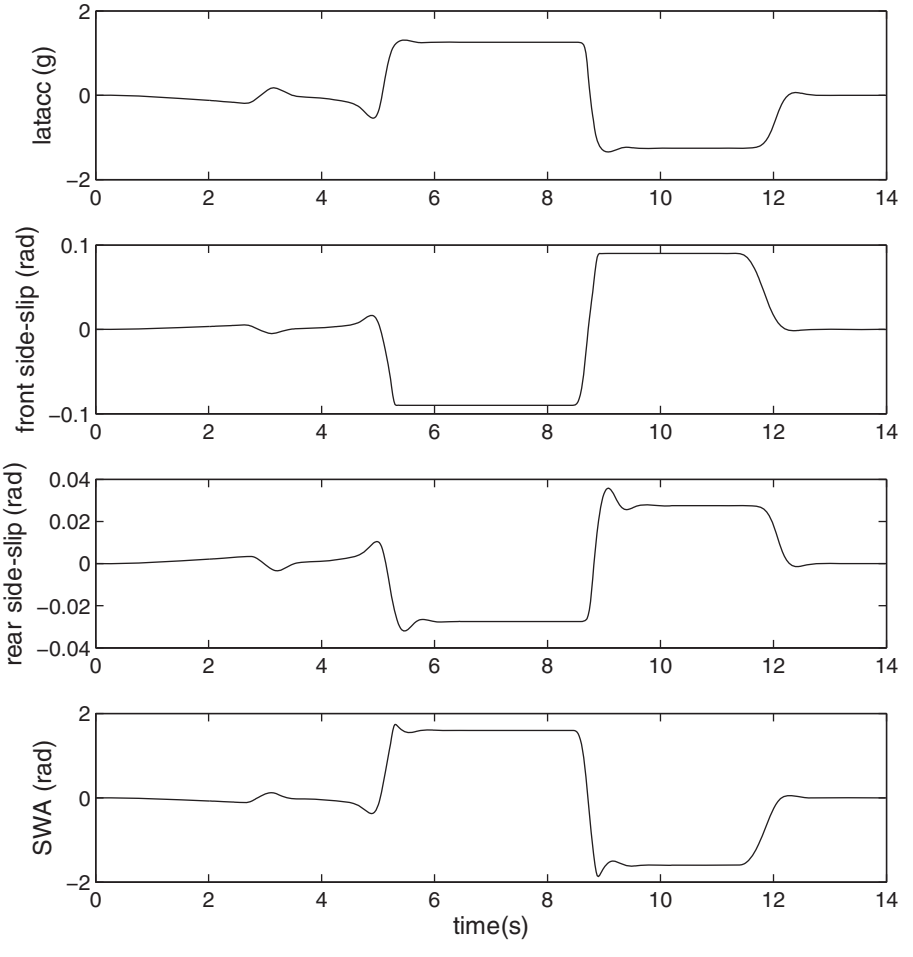

Figure 11. Path optimised time histories for s-bend manoeuvre at 30 ms^{-1}.

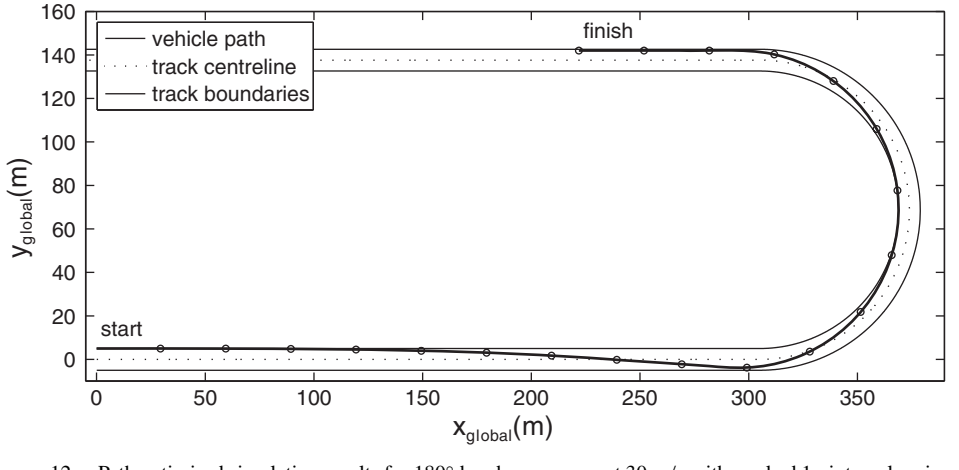

Figure 12. Path optimised simulation results for 180° bend manoeuvre at 30 m/s with marked 1 s intervals using a preview horizon $N_p = 500$.

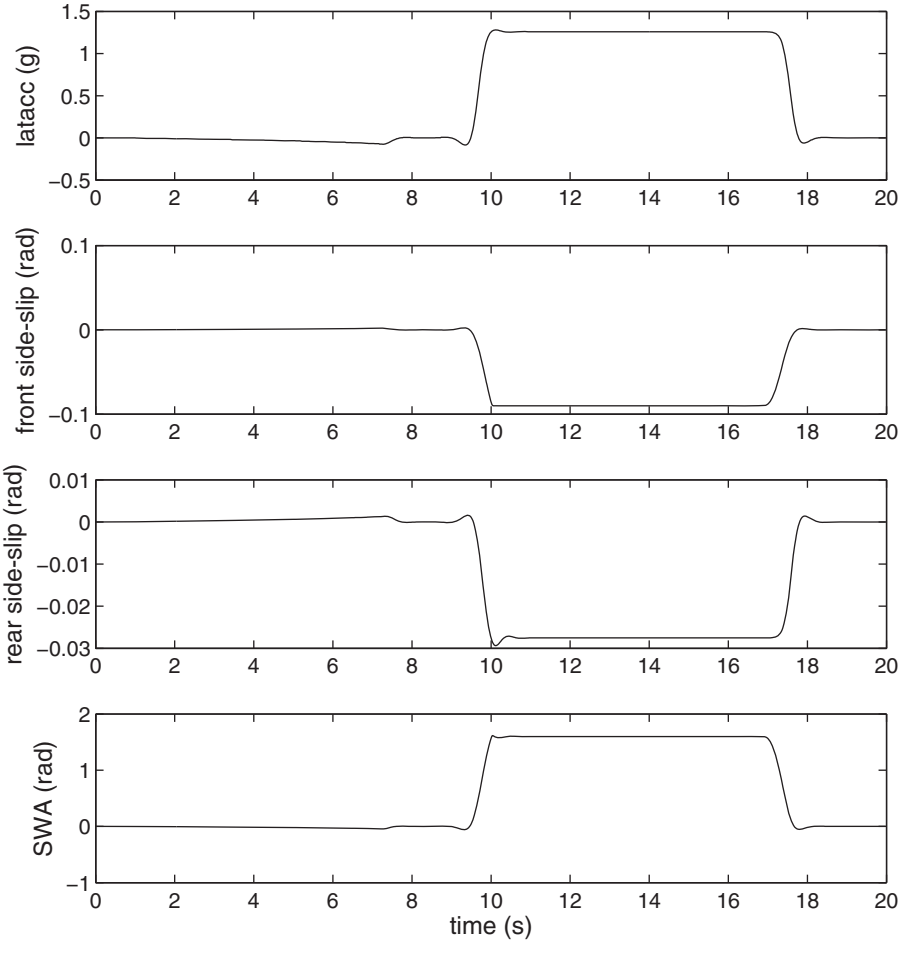

Figure 13. Path optimised time histories for 180° bend manoeuvre at 30 m/s.

part, been motivated by the computational complexity and general fragility of previously developed driver models. The problem has, therefore, been formed in a novel way which results in a computationally efficient and robust optimisation problem. This has been achieved through the use of an LTV vehicle model to approximate the nonlinearities of the tyre lateral force characteristics and an intrinsic coordinate description of the future vehicle and track trajectories. This approach has enabled the geometric positioning of the vehicle relative to the track to be described using linear approximations, resulting in the derivation of a new quadratic path optimisation algorithm. Furthermore, the constraints bounding the permissable vehicle position have been formed as simple linear inequalities. The resultant optimisation problem has thus been simplified to a convex QP problem. To compensate, to some extent, for the prior knowledge a real racing driver is likely to have regarding circuit layout, relatively long control and preview horizons have been used. This has given incentive to adopt an MPC scheme which results in highly structured sparse matrices, reducing computational time significantly when compared to an equally long previewing densely structured approach.

To this extent, a driver model has been developed capable of optimising the path of a nonlinear vehicle through a specified corner sequence, at constant forward speed, in order to minimise the vehicle manoeuvre time. Driver model simulations have demonstrated the

extent to which the approximations in the path optimisation algorithm result in sub-optimal line generation during extreme manoeuvre scenarios. Simulations of more typical manoeuvres have shown that the driver model can successfully operate the vehicle at its lateral limit throughout, minimising the total distance the vehicle travels in order to complete the manoeuvre given the track boundary constraints. However, the constant vehicle forward speed assumption restricts the number of feasible track geometries which result in limit-vehicle operation. Future work therefore includes the extension of the algorithm to combined optimal path and speed profile generation in order to overcome this limitation, together with the control of a more complex vehicle model.

Acknowledgements

The authors gratefully acknowledge the financial contribution of the UK Engineering and Physical Science Research Council and Lotus F1 Team.

References

[1] M. Thommyppillai, S. Evangelou, and R.S. Sharp, *Car driving at the limit by adaptive linear optimal preview control*, Veh. Syst. Dyn. 47(12) (2009), pp. 1535–1550.
[2] M. Thommyppillai, S. Evangelou, and R.S. Sharp, *Advances in the development of a virtual car driver*, Multibody System Dyn. 22 (2009), pp. 245–267.
[3] H. Kwakernaak and R. Sivan, *Linear Optimal Control Systems*, Wiley-Interscience, USA, 1972.
[4] D. Casanova, *On Minimum Time Vehicle Manoeuvring: The Theoretical Optimal Lap*, PhD thesis, School of Mechanical Engineering, Cranfield University, 2000.
[5] D.P. Kelly, *Lap Time Simulation with Transient Vehicle and Tyre Dynamics*, PhD thesis, Cranfield University School of Engineering, 2008.
[6] M. Gerdts, S. Karrenberg, B. Muller-BeBler, and G. Stock, *Generating locally optimal trajectories for an automatically driven car*, Optim. Eng. 10(4) (2009), pp. 439–463.
[7] E. Velenis and P. Tsiotras, *Minimum-time travel for a vehicle with acceleration limits: Theoretical analysis and receding horizon implementation*, J. Optim. Theory Appl. 138(2) (2008), pp. 275–296.
[8] C.C. MacAdam, *Understanding and modeling the human driver*, Veh. Syst. Dyn. 40 (2003), pp. 101–134.
[9] S.D. Keen and D.J. Cole, *Application of time-variant predictive control to modelling driver steering skill*, Veh. Syst. Dyn. 49(4) (2011), pp. 527–559.
[10] J.P. Timings and D.J. Cole, *Minimum manoeuvre time of a nonlinear vehicle at constant forward speed using convex optimisation*, Proceedings of The 10th International Symposium on Advanced Vehicle Control, Loughborough, UK, 2010.
[11] H. Pacejka, *Tyre and Vehicle Dynamics*, Butterworth-Heinemann, Oxford, 2006.
[12] A. Pick and D. Cole, *Neuromuscular dynamics and the vehicle steering task*, Veh. Syst. Dyn. 41 (2004), pp. 182–191.
[13] J. Maciejowski, *Predictive Control with Constraints*, Prentice-Hall, London, 2002.
[14] S.D. Keen, *Modeling Driver Steering Behaviour using Multiple-Model Predictive Control*, PhD thesis, Department of Engineering, University of Cambridge, 2008.
[15] P. Falcone, *Nonlinear Model Predictive Control for Autonomous Vehicles*, PhD thesis, Department of Engineering, University of Sannio, Benevento, 2007.
[16] S. Chang and T. Gordon, *Model-based predictive control of vehicle dynamics*, Int. J. Veh. Autonomous Syst. 5 (2007), pp. 3–27.
[17] S.J. Wright, *Applying new optimization algorithms to model predictive control*, Chemical Process Control-V, CACHE, AIChE Symposium Series No. 316, 93 (1997), pp. 147–155.
[18] C.V. Rao, S.J. Wright, and J.B. Rawlings, *Application of interior-point methods to model predictive control*, J. Optim. Theory Appl. 99 (1998), pp. 723–757.
[19] A. Komatsu, T. Gordon, and M. Best, *Vehicle path optimisation using a time-variant linear optimal reference control*, Proceedings of The 8th International Symposium on Advanced Vehicle Control, Taipei, Taiwan, 2002.